Research Journal of Applied Sciences, Engineering and Technology 6(21): 3946-3952, 2013
DOI:10.19026/rjaset.6.3494
ISSN: 2040-7459; e-ISSN: 2040-7467

Submitted: December 20, 2012 Accepted: January 25, 2013 Published: November 20, 2013

Research Article

Nonlinear Responses of a Two Dimensional Vehicle-pavement System

Shaohua Li and Haoyu Li
Mechanical Engineering School, Shijiazhuang Tiedao University, Shijiazhuang 050043, China

Abstract: The vehicle and pavement are usually investigated separately in vehicle dynamics and pavement dynamics. In this work, a new research scheme is proposed to link the vehicle and pavement model by tire loads and compute the nonlinear dynamic responses by analytical methods. A two-DOF nonlinear vehicle and a Bernoulli-Euler beam on a nonlinear elastic foundation with two simply supported ends compose the nonlinear vehicle-pavement system. The nonlinear tire loads are analytically gained using the averaging method. Then the nonlinear vibration equation of the pavement is obtained using Galerkin method and solved using the multiple scales method. The theoretical solutions are verified by numerical results and the effects of system parameters on pavement vibration are also studied. It is found that the pavement responses excited by tire loads attenuate quickly and small pavement mass, large foundation damping or foundation stiffness may decrease the pavement vibration.

Keywords: Beam on nonlinear elastic foundation, method of multiple scales, nonlinear dynamic, tire loads, vehicle-pavement system

INTRODUCTION

In vehicle dynamics, the responses of vehicles with nonlinear suspensions were widely studied. Stensson *et al*. (1994) analyzed nonlinear phenomena in a vehicle suspension, including multi-solutions, sub-resonance and the system's sensitivity in numerical integral. Li *et al*. (2004) investigated chaos in a hysteretic nonlinear vehicle suspension both by Melnikov method and many numerical methods. Georgios *et al*. (2008) studied the semi-active control based on a nonlinear vehicle with MRF damper. Raghavendra and Pravin (2009) researched the chaotic motion of a one degree of freedom quarter-car model with nonsymmetric potential. However, these researches didn't consider responses of pavement induced by the tire load of a nonlinear vehicle.

In pavement dynamics, responses of a beam or a plate on a nonlinear elastic foundation under moving load was attracted much attention. The moving load is often a constant load or a harmonic load with a fixed frequency. Kargarnovin *et al*. (2005) obtained response of infinite beams supported by nonlinear visco-elastic foundations subjected to harmonic moving loads using a perturbation method and investigated influences of the load speed and frequency on the beam responses. Santee investigated the stability of a beam on nonlinear elastic foundation and obtained the critical boundary of system instability with the method of Melnikov (Santee and Gonalves, 2006). Yang *et al*. (2006) studied nonlinear vibration and singularities of a rectangular thin plate on nonlinear elastic foundation. Xiao *et al*. (2008) investigated bifurcation and chaos of rectangular moderately thick cracked plates on an elastic foundation subjected to periodic load. However the tire load acting on pavement is consist of several frequencies and depends on vehicle suspension vibration. The tire load obtained from vehicle dynamic responses are seldom considered in present studies on pavement dynamics.

In this study, a nonlinear vehicle-pavement system is modeled by a two-DOF nonlinear vehicle and a Bernoulli-Euler beam on the nonlinear elastic foundation. The analytical solutions of wheel and vehicle body displacement are obtained by the averaging method. Then the tire loads of the nonlinear vehicle are gained. Subjected to this tire load, a nonlinear ordinary differential equation of the pavement is obtained using Galerkin method. Then the analytical pavement displacement is gained using the multiple scales method. Effects of system parameters on pavement vibration are also studied, including pavement elastic module, foundation damping, linear foundation stiffness and nonlinear foundation stiffness.

MATHEMATIC MODEL

A nonlinear vehicle-pavement system is modeled by a two-DOF nonlinear vehicle and a Bernoulli-Euler beam on a nonlinear elastic foundation with two simply supported ends, as shown in Fig. 1. It is assumed that the vehicle runs at a constant speed from the midpoint of the beam to right direction.

Corresponding Author: Shaohua Li, Mechanical Engineering School, Shijiazhuang Tiedao University, Shijiazhuang 050043, China, Tel/Fax: 0086-311-87935554

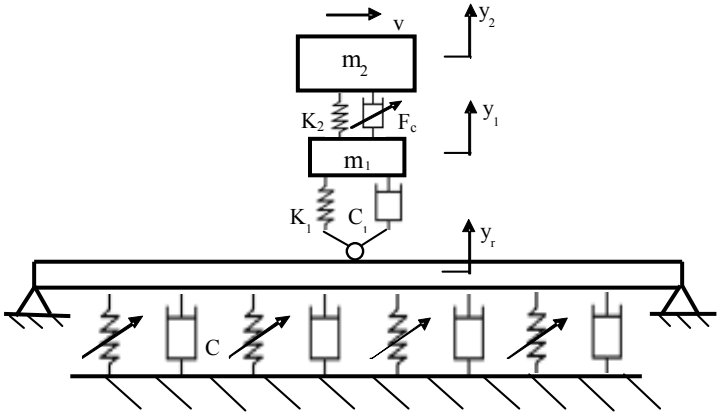

Fig. 1: The nonlinear vehicle-pavement model

The vehicle′s equations of motion are expressed by:

$$\begin{cases} m_1 y_1'' + K_2(y_1 - y_2) - F_c + K_1(y_1 - y_0) + C_1(y_1' - y_0') = 0 \\ m_2 y_2'' + K_2(y_2 - y_1) + F_c = 0 \end{cases} \quad (1)$$

where, m_1, m_2 are the masses of vehicle body and wheel respectively; y_2, y_1 are the body and wheel's vertical displacements respectively; K_1, K_2 are stiffness of tire and suspension, respectively; C_1 is tire's damping coefficient.

The harmonic road roughness y_0 is expressed by:

$$y_0 = B_0 \sin \Omega t \quad (2)$$

where, B_0 is the amplitude of road surface roughness, $\Omega = 2\pi v / L_0$, v and L_0 are the vehicle running speed and the wavelength of road roughness relatively.

F_c is the nonlinear skyhook damping control force of vehicle suspension. A revised Bingham model is applied here (Yang and Li, 2005):

$$F_c = C_2 y_2' + F_y \operatorname{sgn}(y_2' \mp V_0) \quad (3)$$

Here C_2 is the viscous damping coefficient, F_y is controlling force and V_0 is the velocity when MRF damping force is zero.

The vertical vibration equation of the pavement under the moving vehicle loads can be obtained as follows:

$$EI\frac{\partial^4 y_r}{\partial x^4} + K_3 y_r + K_4 y_r^3 + C\frac{\partial y_r}{\partial t} + m\frac{\partial^2 y_r}{\partial t^2} = F\delta(x - L/2 - vt) \quad (4a)$$

where E, I, x, y_r, K_3, K_4, C, L are the modulus of elasticity, cross-sectional moment of inertia, vehicle's position in running direction, beam's vertical displacement, linear foundation stiffness, nonlinear foundation stiffness, foundation damping and the beam's length respectively.

Tire load of the nonlinear vehicle: Letting dimensionless displacement $x_1 = y_1/B_0$, $x_2 = y_2/B_0$ and dimensionless time $\tau = \Omega t$, one gets the dimensionless vehicle system:

$$\begin{cases} \ddot{x}_1 + B_{11}(x_1 - x_2) + B_{12}x_1 + B_{13}\dot{x}_1 - B_{15}\dot{x}_2 - B_{16}\operatorname{sgn}(\dot{x}_2 \mp \dot{x}_{20}) = B_{12}\sin\tau + B_{13}\cos\tau \\ \ddot{x}_2 + B_{21}(x_2 - x_1) + B_{22}\dot{x}_2 + B_{23}\operatorname{sgn}(\dot{x}_2 \mp \dot{x}_{20}) = 0 \end{cases} \quad (4b)$$

where, $\dot{x} = \frac{dx}{d\tau}$, $B_{11} = \frac{K_2}{\Omega^2 m_1}$, $B_{12} = \frac{K_1}{\Omega^2 m_1}$, $B_{13} = \frac{C_1}{\Omega m_1}$, $B_{15} = \frac{C_2}{\Omega m_1}$, $B_{16} = \frac{F_y}{\Omega m_1}$, $B_{21} = \frac{K_2}{\Omega^2 m_2}$, $B_{22} = \frac{C_2}{\Omega m_2}$, $B_{23} = \frac{F_y}{\Omega m_2}$, $\dot{x}_0 = \frac{V_0}{\Omega B_0}$.

Since the coefficients B_{23} are much smaller than other coefficients, the system (4) is weak nonlinear and may be investigated by the averaging method. Letting:

$$\begin{cases} x_i = a_i \cos\varphi_i \\ \dot{x}_i = -a_i \sin\varphi_i \end{cases} \quad (5)$$

where, $\varphi_i = \tau - \theta_i$, $i = 1, 2$.

The averaging equations can be derived as follows:

$$\begin{cases} \dot{a}_1 = P_1 \\ a_1\dot{\theta}_1 = R_1 \\ \dot{a}_2 = P_2 \\ a_2\dot{\theta}_2 = R_2 \end{cases} \quad (6)$$

where,

$$P_1 = \frac{1}{2\pi}\int_0^{2\pi} f_1 \sin\phi_1 d\phi_1$$
$$= \frac{1}{2}B_{11}a_2\sin(\theta_1 - \theta_2) + \frac{1}{2}B_{13}\sin\theta_1 - \frac{1}{2}B_{12}\cos\theta_1 - \frac{1}{2}B_{13}a_1 + \frac{1}{2}B_{15}a_2\cos(\theta_1 - \theta_2)$$

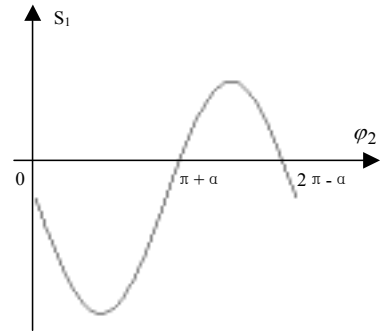

(a) S_1

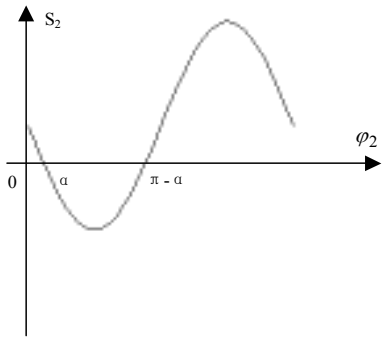

(b) S_2

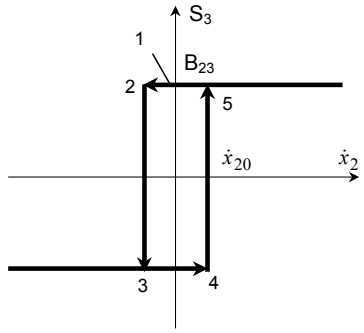

(c) S_3

Fig. 2: Function S_1, S_2 and S_3

$$R_1 = -\frac{1}{2\pi}\int_0^{2\pi} f_1 \cos\phi_1 d\phi_1$$
$$= \frac{1}{2}B_{11}a_2\cos(\theta_1-\theta_2) + \frac{1}{2}B_{13}\cos\theta_1 + \frac{1}{2}B_{12}\sin\theta_1 + \frac{1}{2}(1-B_{11}-B_{12})a_1 - \frac{1}{2}B_{15}a_2\sin(\theta_1-\theta_2)$$

$$P_2 = \frac{1}{2\pi}\int_0^{2\pi} f_2 \sin\varphi_2 d\varphi_2$$
$$= -\frac{1}{2}B_{22}a_2 - \frac{1}{2}B_{21}a_1\sin(\theta_1-\theta_2) + \frac{1}{2\pi}\int_0^{2\pi} B_{23}\,\mathrm{sgn}(-a_2\sin\varphi_2 \mp \dot{x}_{20})\sin\varphi_2 d\varphi_2$$

$$R_2 = -\frac{1}{2\pi}\int_0^{2\pi} f_2 \cos\varphi_2 d\varphi_2$$
$$= \frac{1}{2}(1-B_{21})a_2 + \frac{1}{2}B_{21}a_1\cos(\theta_1-\theta_2) - \frac{1}{2\pi}\int_0^{2\pi} B_{23}\,\mathrm{sgn}(-a_2\sin\varphi_2 \mp \dot{x}_{20})\cos\varphi_2 d\varphi_2$$

$$f_1 = -B_{11}a_2\cos\phi_2 + (B_{11}+B_{12})a_1\cos\phi_1 - B_{13}a_1\sin\phi_1$$
$$- B_{12}\sin\tau - B_{13}\cos\tau + B_{15}a_2\sin\phi_2 - B_{16}\,\mathrm{sgn}(-a_2\sin\phi_2 \mp \dot{x}_{20})$$

$$f_2 = (B_{21}-1)a_2\cos\phi_2 - B_{21}a_1\cos\phi_1 - B_{22}a_2\sin\phi_2 + B_{23}\,\mathrm{sgn}(-a_2\sin\phi_2 \mp \dot{x}_{20})$$

In order to obtain the second term of P_2 and R_2, the following techniques are applied. Letting $S_1 = -a_2\sin\varphi_2 - \dot{x}_{20}$, $S_2 = -a_2\sin\varphi_2 + \dot{x}_{20}$, $S_3 = B_{23}\,\mathrm{sgn}(-a_2\sin\varphi_2 \mp \dot{x}_{20})$. Functions S_1, S_2 and S_3 are shown in Fig. 2.

According to $-\alpha_2\sin\varphi_2 + \dot{x}_{20} = 0$, α is gained:

$$\alpha = \arcsin(\dot{x}_{20}/a_2) \tag{7}$$

The value of φ_2 is 0, α, $\pi-\alpha$, $\pi+\alpha$, and $2\pi-\alpha$ at point 1~5 respectively. The four angles divide a period of 0~2π into five parts. Thus the second term of P_2 and R_2 can be derived:

$$\frac{1}{2\pi}\int_0^{2\pi} B_{23}\,\mathrm{sgn}(-a_2\sin\varphi_2 \mp \dot{x}_{20})\sin\varphi_2 d\varphi_2$$
$$= \frac{B_{23}}{2\pi}\left(\int_0^{\alpha}\sin\varphi_2 d\varphi_2 + \int_{\alpha}^{\pi-\alpha}(-\sin\varphi_2)d\varphi_2 + \int_{\pi-\alpha}^{\pi+\alpha}(-\sin\varphi_2)d\varphi_2\right.$$
$$\left. + \int_{\pi+\alpha}^{2\pi-\alpha}\sin\varphi_2 d\varphi_2 + \int_{2\pi-\alpha}^{2\pi}\sin\varphi_2 d\varphi_2\right)$$
$$= -\frac{2B_{23}}{\pi}\cos\alpha = -\frac{2B_{23}\sqrt{a_2^2-\dot{x}_{20}^2}}{\pi a_2} \tag{8a}$$

$$-\frac{1}{2\pi}\int_0^{2\pi} B_{23}\,\mathrm{sgn}(-a_2\sin\varphi_2 \mp \dot{x}_{20})\cos\varphi_2 d\varphi_2$$
$$= -\frac{B_{23}}{2\pi}\left(\int_0^{\alpha}\cos\varphi_2 d\varphi_2 + \int_{\alpha}^{\pi-\alpha}(-\cos\varphi_2)d\varphi_2 + \int_{\pi-\alpha}^{\pi+\alpha}(-\cos\varphi_2)d\varphi_2\right.$$
$$\left. + \int_{\pi+\alpha}^{2\pi-\alpha}\cos\varphi_2 d\varphi_2 + \int_{2\pi-\alpha}^{2\pi}\cos\varphi_2 d\varphi_2\right)$$
$$= -\frac{2B_{23}}{\pi}\sin\alpha = -\frac{2B_{23}\dot{x}_{20}}{\pi a_2} \tag{8b}$$

Letting $\dot{\alpha}_1 = \dot{\alpha}_2 = \dot{\theta}_1 = \dot{\theta}_2 = 0$, the stable solution equation of system (6) is obtained:

$$B_{11}a_2\sin(\theta_1-\theta_2) + B_{13}\sin\theta_1 - B_{12}\cos\theta_1 - B_{13}a_1 + B_{15}a_2\cos(\theta_1-\theta_2) = 0 \tag{9a}$$

$$B_{11}a_2\cos(\theta_1-\theta_2) + B_{13}\cos\theta_1 + B_{12}\sin\theta_1 + (1-B_{11}-B_{12})a_1 - B_{15}a_2\sin(\theta_1-\theta_2) = 0 \tag{9b}$$

$$\begin{cases} B_{22}a_2 + B_{21}a_1\sin(\theta_1-\theta_2) + \dfrac{4B_{23}\sqrt{a_2^2-\dot{x}_{20}^2}}{\pi a_2} = 0 \\ (1-B_{21})a_2 + B_{21}a_1\cos(\theta_1-\theta_2) - \dfrac{4B_{23}\dot{x}_{20}}{\pi a_2} = 0 \end{cases} \tag{9c, 9d}$$

Eliminating $\theta_1 - \theta_2$ from Eq. (9c) and (9d) yields:

$$(B_{22}a_2\pi + 4B_{23}\sqrt{\frac{a_2^2-\dot{x}_{20}^2}{a_2^2}})^2 a_2^2 + (-\pi a_2^2 + B_{21}\pi a_2^2 - 4\dot{x}_{20}B_{23})^2 = B_{21}^2\pi^2 a_1^2 a_2^2 \tag{10}$$

From Eq. (9c) and Eq. (9d) one has:

$$\begin{cases}\sin(\theta_1-\theta_2)=-(B_{22}\pi a_2^2+4B_{23}\sqrt{a_2^2-\dot{x}_{20}^2})/(B_{21}\pi a_1 a_2)\\ \cos(\theta_1-\theta_2)=[(B_{21}-1)\pi a_2^2+4B_{23}\dot{x}_{20}]/(B_{21}\pi a_1 a_2)\end{cases} \quad (11)$$

Moving the terms including sin θ_1 or cosθ_1 from the left hand of Eq. (9a) and (9b) to the right hand, eliminating θ_1-θ_2 from the two equations and considering Eq. (11), one get:

$$(B_{11}^2+B_{13}^2)a_2^2+(1+B_{11}^2+B_{12}^2+B_{13}^2+2B_{11}B_{12}-2B_{11}-2B_{12})a_1^2+\frac{(2B_{11}-2B_{11}^2-2B_{11}B_{12}-2B_{13}B_{15})}{B_{21}\pi}(-\pi a_2^2+B_{21}\pi a_2^2-4\dot{x}_{20}B_{23})$$
$$+\frac{(2B_{11}B_{13}+2B_{15}-2B_{11}B_{13}-2B_{12}B_{15})}{B_{21}\pi}(B_{22}\pi a_2^2+4B_{23}\sqrt{a_2^2-\dot{x}_{20}^2})=B_{12}^2+B_{13}^2 \quad (12)$$

From Eq. (10) and Eq. (12) one may get a_1 and a_2. Substituting a_1 and a_2 into Eq. (10) leads to θ_1 and θ_2. Thus the analytical displacements of wheel and vehicle body are ascertained:

$$x_1=a_1\cos(\tau-\theta_1),\quad x_2=a_2\cos(\tau-\theta_2) \quad (13)$$

The analytical tire load acting on pavement can be expressed as:

$$F=K_1(y_1-y_0)+C_1(\dot{y}_1-\dot{y}_0)-(m_2+m_1)g=F_1\sin(\Omega t-\theta_1+\theta)-F_2\sin(\Omega t+\theta)-(m_1+m_2)g \quad (14)$$

where,

$$F_1=\sqrt{(K_1B_0a_1)^2+(C_1B_0a_1\Omega)^2},\ F_2=\sqrt{(K_1B_0)^2+(C_1B_0\Omega)^2},\ \theta=\tan^{-1}(C_1\Omega/K_1)$$

Responses of the nonlinear pavement: Letting y_r = U(t) sin πx / L, a nonlinear ordinary equation can be gained as follows:

$$\ddot{U}(t)+\frac{C}{M}\dot{U}(t)+\frac{EI\pi^4+K_3L^4}{ML^4}U(t)+\frac{3K_4}{4M}U(t)^3=F\sin\frac{\pi(L/2+vt)}{L} \quad (15)$$

Substituting the tire load Eq. (14) into Eq. (3), letting dimensionless displacement x_r = U/ B_0 and dimensionless time $\tau = \Omega t$, one get the dimensionless system:

$$\ddot{x}_r+\omega_r^2x_r=-\varepsilon\dot{x}_r-\alpha_3x_r^3+\alpha\cos(\gamma_1\tau+\theta_1)+\alpha\cos(\gamma_2\tau+\theta_1)+\alpha_6\cos\gamma\tau \quad (16)$$

where,

$\omega_r=\sqrt{(EI\pi^4+KL^4)/(\Omega^2ML^4)}$
$\varepsilon=C/(M\Omega)$
$\alpha_3=3K_2B_0^2/(4M\Omega^2)$
$\alpha=\sqrt{\alpha_4^2+\alpha_5^2}/2,$
$\theta_1=\tan^{-1}(\alpha_5/\alpha_4-\pi/2),$
$\alpha_6=-(m_1+m_2)g/(B_0^2M\Omega^2)$
$\gamma_1=1+L_0/(2L),\quad \gamma_2=1-L_0/(2L)\ \gamma=L_0/(2L)$

Here

$$\alpha_4=(F_1\cos(\phi+\theta)-F_2\cos\theta)/(B_0M\Omega^2)$$
$$\alpha_5=(F_1\sin(\phi+\theta)-F_2\sin\theta)/(B_0M\Omega^2)$$

Due to the weak nonlinearity of system (16), the responses can be gained by the multiple scale method. Since the excitation frequency is much smaller than the inherence frequency of system (16), only the non-resonance condition is considered.

One may express the solution in terms of different time scales as:

$$x_r(t)=x_{r0}(T_0,T_1)+\varepsilon x_{r1}(T_0,T_1) \quad (17)$$

where, $T_0=\tau$, $T_1=\varepsilon\tau$.

Substituting Eq. (17) into Eq. (16) and equating coefficients of like powers of ε leads to:

$$\begin{cases}D_0^2x_{r0}+\omega_r^2x_{r0}=\alpha\cos(\gamma_1T_0+\theta_1)+\alpha\cos(\gamma_2T_0+\theta_1)+\alpha\cos(\gamma T_0)\\ D_0^2x_{r1}+\omega_r^2x_{r1}=-2D_0D_1x_{r0}-D_0x_{r0}-\alpha_3x_{r0}^3\end{cases} \quad (18)$$

The solution for the first line of Eq.(18) is given the form:

$$x_{r0}(T_0,T_1)=A(T_1)e^{j\omega_rT_0}+B_1e^{jr_1T_0}+B_2e^{jr_2T_0}+B_3e^{jrT_0}+cc \quad (19)$$

where, *cc* denotes the complex conjugate of the preceding terms and $A=ae^{j\beta}/2$, $B_1=\alpha e^{j\theta_1}/(\omega_r^2-\gamma_1^2)$, $B_2=\alpha e^{j\theta_2}/(\omega_r^2-\gamma_2^2)$, $B_3=\alpha/(\omega_r^2-\gamma^2)$.

Substituting Eq. (19) into the second line of Eq. (18) leads to the condition for eliminating the secular term:

$$-3\alpha_3A^2\bar{A}-2j\omega_rD_1A-j\omega_rA-6\alpha_3AB_1\bar{B}_1-6\alpha_3AB_2\bar{B}_2-6\alpha_3AB_3\bar{B}_3=0 \quad (20)$$

Separating the real and imaginary parts of Eq. (20), one obtains:

$$\begin{cases}D_1a=-\frac{1}{2}a\\ D_1\beta=\frac{3\alpha_3}{8\omega_r}(a^2+2B_1^2+2B_2^2+2B_3^2)\end{cases} \quad (21)$$

From Eq. (21), one can get the first order approximate solution of the dimensionless system (16):

$$x_r(t)=\alpha\cos(\omega_r\tau+\beta)+B_1\cos(\gamma_1\tau+\theta_1)+B_2\cos(\gamma_2\tau+\theta_1)+B_3\cos(\gamma\tau) \quad (22)$$

where,

$$a=c_1e^{-T_1/2},\ \beta=3\alpha_3(-c_1^2e^{-T_1}+2B_1^2T_1+2B_2^2T_1+2B_3^2T_1)/8\omega_r+c_2$$

Thus the analytical pavement displacement under the moving vehicle loads is gained:

$$y_r=B_0x_r(t)\sin\pi x/L \quad (23)$$

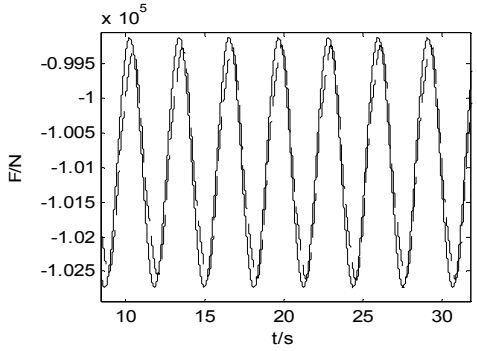

Fig. 3: Numerical verification of the analytical tire load

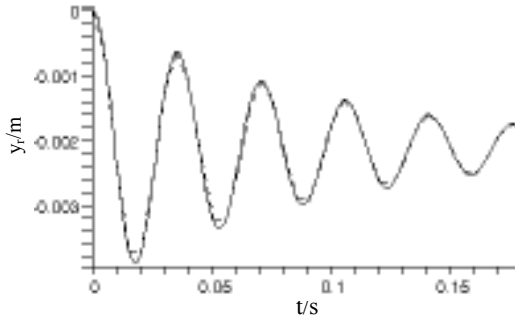

Fig. 4: The theoretical solution and numerical solution of pavement displacement

Numerical simulation: Parameters of the nonlinear vehicle-pavement system (Wang *et al*., 2005; Deng, 2000) are m_2 = 10109 kg, m_1 = 190 kg, K_1 = 2060000 N/m, C_1 = 900 Ns^2/m, K_2 = 75000 N/m, C_2 = 9000 Ns^2/m, C_3 = 1000 Ns^2/m, v_0 = 0.1, F_y = 1000 N, B_0 = 0.5 m, Ω = 2Hz, L_0 = 20 m, $E = 1.6\times10^9$ N/m^2, $I = 5\times10^{-4}$m^4, $K_3 = 48\times10^6$ N/m^2, $K_4 = -4.8\times10^6$ N/m^2, $C = 0.3\times10^5$ Ns/m^2, M = 1500 Kg, L = 120 m.

To verify the analytical tire load from averaging method, the numerical tire load is obtained by the Rugga-Kutta method according to Eq. (1), as shown in the dashed line in Fig. 3. The solid line is the analytical tire load calculated by Eq. (14). From Fig. 3 it can be seen that the analytical tire load is very near to the numerical one. Thus the analytical tire load can be used to investigate the pavement response.

The solid line in Fig. 4 shows the analytical solution of the pavement displacement obtained by Eq. (23). The dashed line From Fig. 4 in Fig. 4 is the numerical pavement displacement obtained by integrating Eq. (16) numerically. It can be found that the pavement response excited by vehicle loads attenuates quickly and the analytical pavement displacement is very near to the numerical one. Thus the verification of the analytical pavement response Eq. (23) is tested.

Varying the road excitation frequency Ω from 0.5 rad/s to 22 rad/s, the amplitude frequency response curve of pavement displacement is gained from Eq. (23), as shown in Fig. 5. It can be seen from Fig. 5 that with the rise of the road excitation frequency, two peaks occur in the pavement response which is associate with the inherence frequency of the vehicle body and the tire. Letting L0 = 10 m, these two peak will occur at the running speed 14km/h and 100 km/h. Thus it can be concluded that as the running speed increases, the increase in road vibration is not monotonous. In other words, the heavy vehicle running at low speed may lead to more severe road vibration than that running at high speed.

Figure 6 shows the effects of six system parameters on pavement vibration, including pavement length, pavement mass, elastic modulus, foundation damping, linear foundation stiffness and nonlinear foundation stiffness. It can be seen that

- With the rise of pavement length or pavement mass, the amplitude of pavement displacement increases. Large elastic modulus, foundation damping or foundation stiffness will reduce pavement vibration.

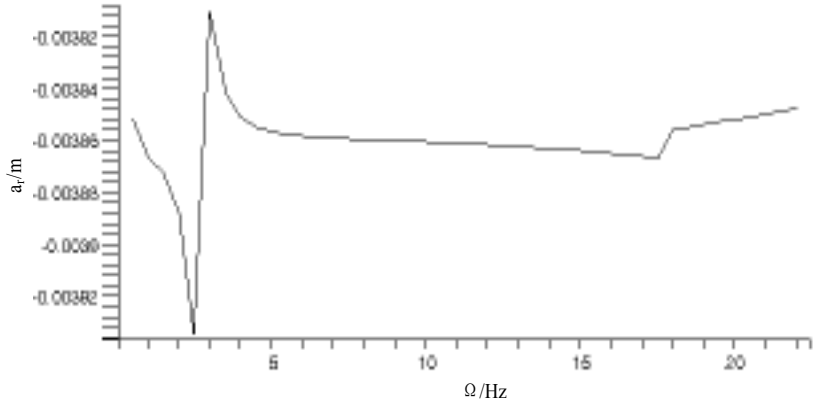

Fig. 5: The amplitude frequency response curve of pavement displacement

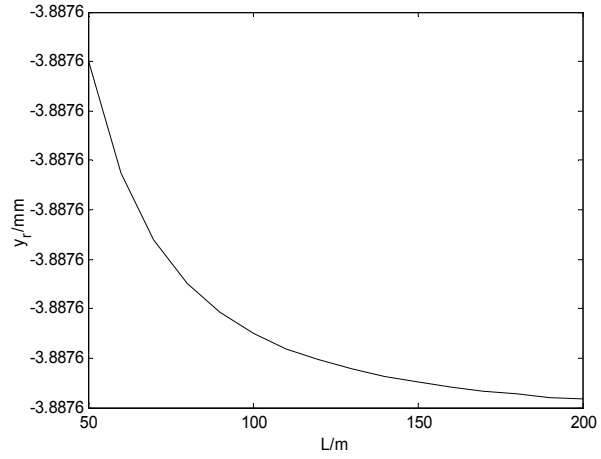

(a) The effect of pavement length

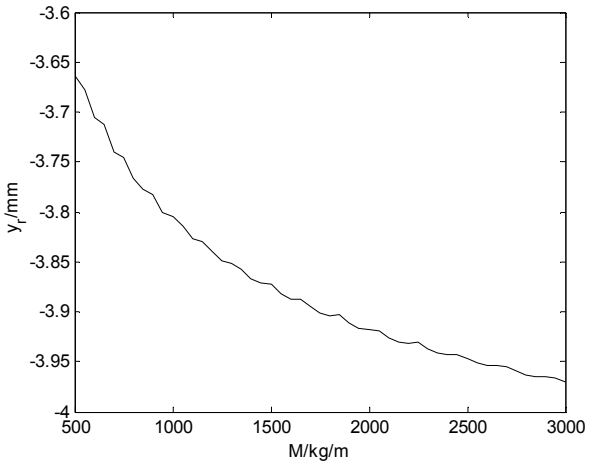

(b) The effect of pavement mass

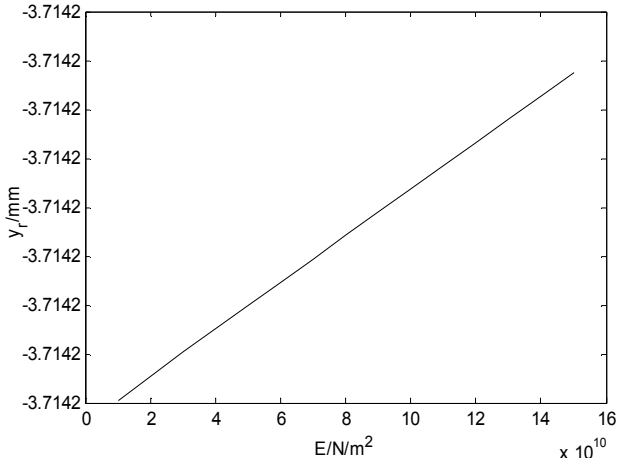

(c) The effect of elastic modulus

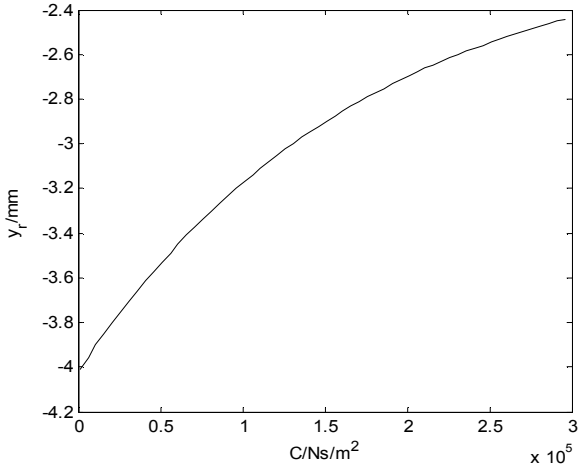

(d) The effect of foundation damping,

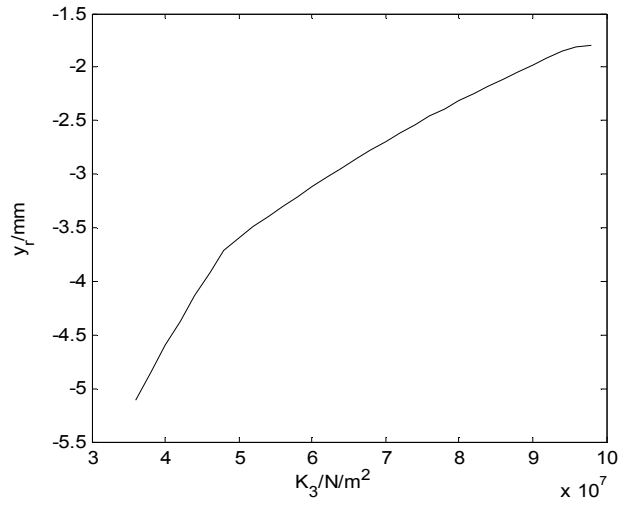

(e) The effect of foundation stiffness

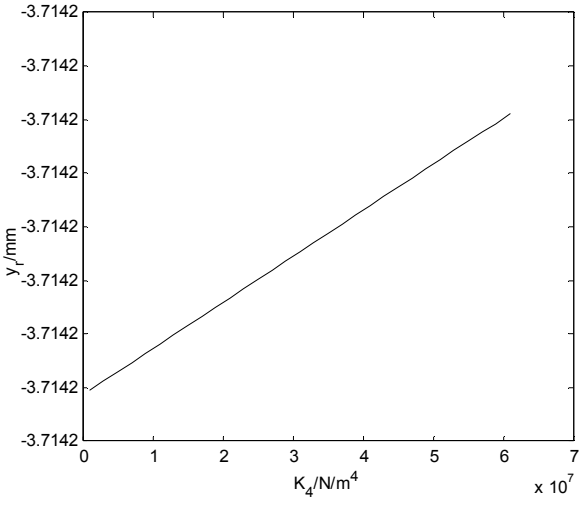

(f) The effect of nonlinear foundation stiffness

Fig. 6: The effect of system parameters on pavement vibration

- The effect of pavement mass, foundation damping and foundation stiffness is greater than that of the other three parameters.

CONCLUSION

Nonlinear dynamics of a vehicle-pavement system is investigated with the method of averaging, Galerkin and multiple scales. Some numerical results are presented as well. It can be concluded from this work that:

- The analytical solutions of nonlinear vehicle using averaging method can be used to compute the tire load acting on pavement with enough accuracy.
- The pavement response excited by vehicle loads attenuate quickly and the heavy vehicle running at low speed may lead to more severe vibration than that running at high speed.
- Small pavement mass, large foundation damping or foundation stiffness may decrease the amplitude of pavement vibration.

ACKNOWLEDGMENT

The National Natural Science Foundation of China under Grant No. 11072159, 11102121 and the Natural Science Foundation of Hebei province under Grant No. E2012210025, E2011210055 support this study.

REFERENCES

Deng, X.J., 2000. Subgrade and Pavement Engineering. China Communications Press, Beijing.

Georgios, T., W.S. Charles and G. Emanuele, 2008. Hybrid balance control of a magnetorheological truck suspension. J. Sound Vib., 317(3-5): 514-536.

Kargarnovin, M.H., D. Younesian and D.J. Thompson, 2005. Response of beams on nonlinear viscoelastic foundations to harmonic moving loads. Comput. Struct., 83(2005): 1865-1877.

Li, S.H., S.P. Yang and W.W. Guo, 2004. Investigation on chaotic motion in hysteretic nonlinear suspension system with multi-frequency excitation. Mech. Res. Commun., 31: 229-236.

Raghavendra D.N. and M.S. Pravin, 2009. Establishing the limiting conditions of operation of magneto-rheological fluid dampers in vehicle suspension systems. Mech. Res. Commun., 36: 957-962.

Santee, D.M. and P.B. Gonalves, 2006. Oscillations of a beam on a non-linear elastic foundation under periodic loads. Shock Vib., 13(4-5): 273-284.

Stensson, A., C. Asplund and L. Karlsson, 1994. Nonlinear behaviour of a MacPherson strut wheel suspension. Vehicle Syst. Dyn., 23(2): 85-106.

Wang, J.J., W. Zhang and W.X. Wu, 2005. Analysis of dynamic response of simply supported girder bridge under heavy moving vehicles. Central South Highway Eng., 30(2): 55-62.

Xiao Y.G., Y.M. Fu and X.D. Zhao, 2008. Bifurcation and chaos of rectangular moderately thick cracked plates on an elastic foundation subjected to periodic load. Chaos. Soliton. Fract., 35(3): 460-465.

Yang, S.P. and S.H. Li, 2005. A hysteresis model for MR damper. Int. J. Nonlin. Sci. Num., 6(2): 139-144.

Yang, Z.A., X.J., Zhao and X.Y. Xiao, 2006. Nonlinear vibration and singularities analysis of a thin rectangular plate on nonlinear elastic foundation. J. Vib. Shock, 25(5): 69-73.